



Published in final edited form as:

Inorg Chem Commun. 2015 September 1; 59: 71–75. doi:10.1016/j.inoche.2015.07.002.

Synthesis, structural studies, and oxidation catalysis of the manganese(II), iron(II), and copper(II) complexes of a 2-pyridylmethyl pendant armed side-bridged cyclam

Anthony D. Shircliff¹, Kevin R. Wilson¹, Desiray J. Cannon¹, Donald G. Jones¹, Zhan Zhang², Zhuqi Chen², Guochuan Yin², Timothy J. Prior³, and Timothy J. Hubin¹

¹Department of Chemistry and Physics, Southwestern Oklahoma State University, 100 Campus Drive, Weatherford, OK 73096

²Key Laboratory for Large-Format Battery Materials and System, Ministry of Education, School of Chemistry and Chemical Engineering, Hubei Key Laboratory of Material Chemistry and Service Failure, Huazhong University of Science and Technology, Wuhan 430074, PR China

³Department of Chemistry, The University of Hull, Cottingham Road, Hull, UK, HU6 7RX

Abstract

The first 2-pyridylmethyl pendant armed structurally reinforced cyclam ligand has been synthesized and successfully complexed to Mn²⁺, Fe²⁺, and Cu²⁺ cations. X-ray crystal structures were obtained for the diprotonated ligand and its Cu²⁺ complex demonstrating pentadentate binding of the ligand with *trans-II* configuration of the side-bridged cyclam ring, leaving a potential labile binding site *cis* to the pyridine donor for interaction of the complex with oxidants and/or substrates. The electronic properties of these complexes were determined by means of solid state magnetic moment, with a low value of $\mu = 3.10 \mu_B$ for the Fe²⁺ complex suggesting it has a trigonal bipyramidal coordination geometry, matching the crystal structure of the Cu²⁺ complex, while the $\mu = 5.52 \mu_B$ value for the Mn²⁺ complex suggests it is high spin octahedral. Cyclic voltammetry in acetonitrile revealed reversible redox processes in all three complexes, suggesting catalytic reactivity involving electron transfer processes are possible for these complexes. Screening for oxidation catalysis using hydrogen peroxide as the terminal oxidant identified the Fe²⁺ complex as the oxidation catalysts most worthy of continued development.

Keywords

structurally reinforced cyclam; side-bridged cyclam; pendant-arm macrocycle; oxidation catalysis; 2-pyridylmethyl

We have studied cross-bridged cyclam complexes of manganese and iron for nearly a decade and a half as oxidation catalysts. [1] [2] [3] [4] [5] [6] [7] [8] [9] [10] [11] [12] [13]

Correspondence to: Guochuan Yin; Timothy J. Prior; Timothy J. Hubin.

Publisher's Disclaimer: This is a PDF file of an unedited manuscript that has been accepted for publication. As a service to our customers we are providing this early version of the manuscript. The manuscript will undergo copyediting, typesetting, and review of the resulting proof before it is published in its final citable form. Please note that during the production process errors may be discovered which could affect the content, and all legal disclaimers that apply to the journal pertain.

[14] The manganese complex of 4,11-dimethyl-1,4,8,11-tetraazabicyclo[6.6.2]hexadecane [15] (**Me₂EBC**, Scheme 1) in particular, has a rich oxidation chemistry. [5] [6] [7] [8] [9] [10] [11] [12] [13] [14] This compound, which we propose to call “the Busch catalyst”, was initially synthesized as an oxidation catalyst because the cross-bridged ligand could rigidly bind the oxygen-reactive manganese metal and stop it from being lost in the form of MnO₂. [1] [2] [3] [4] Que has determined that the iron complex of **Me₂EBC** is an efficient olefin epoxidation catalyst with H₂O₂ oxidant under appropriate conditions as well. [16]

Cyclam ligands structurally reinforced with an ethylene bridge between nitrogens 1 and 4 (i.e. “side-bridged”) have been known since 1980. [17] [18] [19] [20] [21] [22] [23] [24] [25] [26] The additional bridge provides rigidity, configurational selectivity, and kinetic stability and has been synthetically put in place by several different methods. [17] [18] [19] [20] [21] Like other cyclam ligands, additional utility can be added by addition of pendant arms, which have included in Scheme 1, **structure 1**: R and/or R' = H, [17] [21] Me, [19] Et, [20] Bz, [19] [23] [22]Bz-*p*-NO₂, [22] [25]Bz-*p*-NH₂, [22] CH₂CO₂H, [24] [26]CH₂PO₃H [25] [26] and others.

An interesting 2-pyridylmethyltrimethylcyclam ligand (Scheme 1, **structure 2**) was reported by Que and coworkers [27] and stimulated our present work. Its iron complex activated dioxigen and formed an oxoiron(IV)intermediate that was crystallographically characterized, but has not been pursued further as a catalyst. [27] Although 2-pyridylmethyl pendant armed unbridged cyclams are ubiquitous, [28] [29] [30] [31] [32] [33] [34] [35] [36] [37] [38] no 2-pyridylmethyl pendant armed side-bridged or cross-bridged cyclams had been reported prior to our work. Due to our experience with bridged cyclam oxidation catalysts, we set out to synthesize and characterize side- and cross-bridged cyclam ligands containing a 2-pyridylmethyl pendant arm, along with their most biologically relevant oxidation active metal ion complexes: manganese, iron, and copper. Our cross-bridged work has been reported elsewhere. [39] Here, we report on the results of our efforts with the side-bridged cyclam ligand, (Scheme 1, **structure 3**) and the screening of its complexes as potential oxidation catalysts.

Alkylation of the cyclam-glyoxal bisaminal **4** in typical S_N2 solvents like acetonitrile was unsuccessful due to self-reaction of the picolyl chloride. So, we explored the chlorinated solvents [40] to stabilize this reagent in the presence of the bisaminal and found successful, although low- yielding, monoalkylation with picolyl chloride in chloroform at room temperature. [41] We raised the yields of the monoalkyl salt **5** to 66% by addition of KI and increasing the temperature to reflux over 6 days. Typical reduction conditions [23] gave **3** in good yield. Metal complexation with anhydrous metal chlorides in dry solvents under nitrogen gave adequate yields of the desired complexes. [41]

The X-ray crystal structures of the H₂**3**Cl₂ • 2 H₂O and [Cu(**3**)]PF₆]₂ • C₃H₆O were obtained and are depicted in Figure 1. [42] The ligand is protonated at one of the piperazine tertiary nitrogens, and at the secondary nitrogen of the cyclam ring. There is an extensive hydrogen bonding network between the chloride anions, the two waters of crystallization, the cyclam nitrogens, and their protons. The pyridine nitrogen is oriented away from the center of the cyclam ring and is not involved in the hydrogen bonding network.

Upon coordination of Cu^{2+} , the pyridine nitrogen is oriented into the center of the cyclam ring and coordinates the Cu^{2+} ion located there. This compound contains Cu^{2+} in two different coordination geometries. The ligand coordinates through each of the nitrogen atoms but in a slightly different orientation. The two copper complexes are approximately enantiomers, as shown in Figure 1(c). The coordination geometry around the copper(II) ion is somewhat between trigonal bipyramidal (as shown in Figure 1(b)) and square pyramidal (as shown in Figure 1(c)). To illustrate the slight differences between the two different metal ion coordination geometries of this structure, square pyramidal type bond angles for the two different copper(II) ions are given: Cu(1) N–Cu–N angles / °: (in plane) 100.9(2), 74.0(2), 94.75(19), 87.79(19); (to N5) 82.91(17), 118.02(18), 101.94(17), 97.03(18). Cu(2) N–Cu–N angles / °: (in plane) 102.10(19), 73.4(2), 91.7(2), 86.2(2); (to N25) 80.5(2), 107.85(18), 107.37(19), 120.5(2). Complete metrical parameters for both structures are given in the Supplementary Information.

Unfortunately, crystal structures of the Mn^{2+} and Fe^{2+} complexes were not obtained. We sought other hints at their structures and turned to solid state magnetic moments to help determine them. First, the magnetic moment of $[\text{Cu}(\mathbf{3})][\text{PF}_6]_2$ was determined to be $2.32 \mu_{\text{B}}$, which is consistent with $n = 1$ for a $d^9 \text{Cu}^{2+}$ ion. [43] $[\text{Mn}(\mathbf{3})\text{Cl}]\text{PF}_6$ was determined to have $\mu = 5.52 \mu_{\text{B}}$, which is consistent with $n = 5$ for a high spin octahedral $d^5 \text{Mn}^{2+}$ metal ion. [43] High spin $n = 5$ is not diagnostic of a particular coordination geometry for Mn^{2+} , but the consistent presence of one chloride in the elemental analysis of this complex led us to conclude that the most likely structure is a 6-coordinate pseudo-octahedral one. If the chloride is not coordinated and the complex is only 5-coordinate, precipitation by PF_6^- would have led to the dihexafluorophosphate salt.

Perhaps the most interesting contribution to structural information came from the magnetic moment of $[\text{Fe}(\mathbf{3})\text{Cl}_2]$. $\mu = 3.10 \mu_{\text{B}}$, which is most consistent with $n = 2$ for a low spin 5-coordinate $d^6 \text{Fe}^{2+}$ metal ion. [44] In our previous experience with Mn^{2+} and Fe^{2+} complexes of bridged tetraazamacrocycles, [1] [3] [45] both ions agree in that they were high spin and 6-coordinate. However, in this case, $\text{Mn}(\mathbf{3})\text{Cl}^+$ appears 6-coordinate and high spin, while $\text{Fe}(\mathbf{3})^{2+}$ appears 5-coordinate and low spin. Two supporting pieces of evidence for this perhaps unexpected geometry for the Fe^{2+} complex are (1) the 5-coordinate $\text{Cu}(\mathbf{3})^{2+}$ crystal structure presented above for this ligand system; and (2) an unpublished crystal structure in which Fe^{2+} is coordinated to the four nitrogens of a similar ethylene side-bridged ligand having a methyl group in place of the pyridylmethyl group of $\mathbf{3}$, and a chloro ligand. [39] Interestingly, a six-coordinate 1,8-bispyridylmethylcyclam Fe^{2+} complex with spin-crossover properties and a transition temperature to low spin of 150 K is known. [46] Of course, low spin $d^6 \text{Fe}^{2+}$ complexes are ubiquitous in organometallic chemistry. A number of 5-coordinate low-spin Fe^{2+} examples have been published. [47] [48] [49] [50]

In anticipation of carrying out oxidation studies, we obtained cyclic voltammograms (Figure 2) on these complexes in acetonitrile looking for multiple stabilized oxidations states if catalytic processes were to be likely. Unfortunately, only one reversible redox wave was observed for each complex. Relative to SHE, $\text{Cu}(\mathbf{3})^{2+}$ gave a reversible $\text{Cu}^{1+/2+}$ redox wave at $E_{1/2} = -0.586 \text{ V}$ ($E = 77 \text{ mV}$). No oxidation to Cu^{3+} was observed, which is perhaps not surprising, as there are no negatively charged ligands to help stabilize the Cu^{3+} cation.

$\text{Cu}(\text{Me}_2\text{EBC})\text{Cl}^+$ has an irreversible Cu^{2+} to Cu^+ reduction wave at $E_{\text{red}} = -0.544$ V and an irreversible Cu^{2+} oxidation to Cu^{3+} at $E_{\text{ox}} = +1.530$ V. [51] In comparison, $\text{Cu}(\mathbf{3})^{2+}$ is more difficult to oxidize (due to lack of negatively charged ligands) and more reversibly reduced.

$\text{Mn}(\mathbf{3})\text{Cl}^+$ gave a reversible $\text{Mn}^{2+/3+}$ redox wave at $E_{1/2} = +0.856$ V ($E = 93$ mV) and an irreversible reduction at $E_{\text{red}} = -0.685$ V. This can be compared to the well-known $\text{Mn}(\text{Me}_2\text{EBC})\text{Cl}_2$ catalyst [1] which has reversible $\text{Mn}^{2+/3+}$ and $\text{Mn}^{3+/4+}$ waves at $E_{1/2} = +0.585$ V ($E = 61$ mV) and $E_{1/2} = +1.343$ ($E = 65$ mV), respectively. The single chloro ligand allows only Mn^{3+} to be accessed for $\text{Mn}(\mathbf{3})\text{Cl}^+$, and at a higher potential, since only one negatively charged chloro ligand is present to stabilize the growing positive charge. Reduction is possible here, when not observed for $\text{Mn}(\text{Me}_2\text{EBC})\text{Cl}_2$, but not reversible, likely due to the loss of the chloro ligand upon reduction to Mn^+ .

5-coordinate $\text{Fe}(\mathbf{3})^{2+}$ exhibits a complex cyclic voltammogram with a reversible $\text{Fe}^{2+/3+}$ wave at $E_{1/2} = +0.456$ V ($E = 78$ mV), two irreversible reductions at $E_{\text{red}} = -0.802$ V and -1.671 V, respectively, and a large return oxidation at $E_{\text{ox}} = -0.252$ V. A much simpler behavior is observed for $\text{Fe}(\text{Me}_2\text{EBC})\text{Cl}_2$, with only $E_{1/2} = 0.110$ ($E = 63$ mV) observed for $\text{Fe}^{2+/3+}$. [1] Oxidation is obviously much easier for the latter complex, where two negatively charged chloro ligands stabilize the positive charge. Reduction is observed only for $\text{Fe}(\mathbf{3})^{2+}$, where no negatively charge ligands inhibit it. The complex behavior of $\text{Fe}(\mathbf{3})^{2+}$ after the initial reduction is the subject of ongoing study.

Finally, we present initial oxidation screening data on these complexes. As shown in Table 1, compared with its analog, $\text{Mn}(\text{Me}_2\text{EBC})\text{Cl}_2$ complex, the redox activities of $\text{Cu}(\mathbf{3})^{2+}$, and $\text{Mn}(\mathbf{3})\text{Cl}^+$ are quite poor. In sulfide oxidation using H_2O_2 as oxidant, while the $\text{Mn}(\text{Me}_2\text{EBC})\text{Cl}_2$ catalyst provided nearly complete conversion of thioanisole (99.8%) with 44.3% yield of sulfoxide and 46.5% of sulfone, the $\text{Cu}(\mathbf{3})^{2+}$ and $\text{Mn}(\mathbf{3})\text{Cl}^+$ complexes are almost inactive for sulfide oxidation. However, $\text{Fe}(\mathbf{3})^{2+}$ demonstrated some activity, providing 9.7% yield of sulfoxide, and 2.9% of sulfone with 15.6% conversion. Similarly, in hydrogen abstraction from 1,4-cyclohexadiene, $\text{Mn}(\text{Me}_2\text{EBC})\text{Cl}_2$ gave 71.4% yield of benzene with 86.2% conversion, and $\text{Cu}(\mathbf{3})^{2+}$ and $\text{Mn}(\mathbf{3})\text{Cl}^+$ complexes were still inactive for benzene formation ($\sim 3\%$ yields represent natural benzene content in commercial 1,4-cyclohexadiene). Again, $\text{Fe}(\mathbf{3})^{2+}$ provides more encouraging results, generating 23.6% yield of benzene with 44.5% conversion.

These results are perhaps not surprising, when reconciled with the electrochemical studies (Figure 2). $\text{Mn}(\mathbf{3})\text{Cl}^+$ has only a redox couple of $\text{Mn}^{2+/3+}$ at $E_{1/2} = +0.856$ V, which is much higher than that of the corresponding $\text{Mn}^{2+/3+}$ couple of $\text{Mn}(\text{Me}_2\text{EBC})\text{Cl}_2$ ($E_{1/2} = +0.585$ V), and no access to Mn(IV). Therefore, the catalytic cycle of the $\text{Mn}(\mathbf{3})\text{Cl}^+$ complex is very sluggish in oxidations. Similar sluggish redox behavior is observed in $\text{Cu}(\mathbf{3})^{2+}$ since its oxidation to $\text{Cu}(\mathbf{3})^{3+}$ is not observed. For the $\text{Fe}(\mathbf{3})^{2+}$ complex, although its catalytic activity in sulfide oxidation, an oxygen transfer process, is poor, it still demonstrates a relatively good activity in hydrogen abstraction because its redox couple for $\text{Fe}^{2+/3+}$ is modest ($E_{1/2} = +0.456$ V) and even lower than that of $\text{Mn}(\text{Me}_2\text{EBC})\text{Cl}_2$. Consistent with the hydrogen abstraction activity of the $\text{Fe}(\mathbf{3})^{2+}$ complex, Stack has reported[55] that $\text{Fe}(\text{PY5})(\text{OH})^{3+}$, which has a potential of $E_{\text{pc}} = +0.555$ V, is capable of stoichiometric hydrogen abstraction

from 9,10-dihydroanthracene (**PY5** = 2,6-bis-(bis(2-pyridyl)methoxymethane)pyridine). This result encourages us to continue the exploration of the $\text{Fe}(\mathbf{3})^{2+}$ complex and its biological relevance to lipoxygenase[56] in the future.

In conclusion, a new pyridylmethyl N-pendant arm, side-bridged cyclam ligand, **3**, has been synthesized, and its diprotonated salt structurally characterized, with a key synthetic step the use of non-polar chloroform to decrease the self-reactivity of picolyl chloride in the presence of bisaminal **4**. Divalent Mn, Fe, and Cu complexes were synthesized and the copper(II) complex structurally characterized by X-ray crystallography as 5-coordinate $\text{Cu}(\mathbf{3})^{2+}$ showing the cyclam ring of **3** in a *trans*-II configuration and the chelated pyridine nitrogen bound to the Cu^{2+} ion. Solid state magnetic moment determination and elemental analysis revealed a high spin, octahedral $\text{Mn}(\mathbf{3})\text{Cl}^+$ cation, but a 5-coordinate, low-spin $\text{Fe}(\mathbf{3})^{2+}$ cation. Electrochemical studies in acetonitrile revealed reversible access to only two oxidation states for each metal ion, whereas optimal behavior for successful oxidation catalysis is likely a greater redox range. Preliminary screens for oxidation catalysis using H_2O_2 as the oxidant carried out on all three complexes showed promising results only in the hydrogen atom abstraction of 1,4-cyclohexadiene by $\text{Fe}(\mathbf{3})^{2+}$, which is consistent with another iron complex from the literature having a similar redox potential. [55] Future work will include expanding the range of oxidation reactions possible with this catalyst and determination of its oxidation catalysis mechanisms.

Supplementary Material

Refer to Web version on PubMed Central for supplementary material.

Acknowledgments

TJH acknowledges the Donors of the American Chemical Society Petroleum Research Fund; Health Research award for project number HR13-157, from the Oklahoma Center for the Advancement of Science and Technology; and Grant Number P20RR016478 from the National Center for Research Resources (NCRR), a component of the National Institutes of Health (NIH) for partial support of this research. TJH also acknowledges the Henry Dreyfus Teacher-Scholar Awards Program for support of this work.

References

1. Hubin TJ, McCormick JM, Collinson SR, Buchalova M, Perkins CM, Alcock NW, Kahol PK, Raghunathan A, Busch DH. *J Am Chem Soc.* 2000; 122:2512–2522.
2. Hubin TJ, McCormick JM, Alcock NW, Busch DH. *Inorg Chem.* 2001; 40:435–444. [PubMed: 11209599]
3. Hubin TJ, McCormick JM, Collinson SR, Alcock NW, Clase HJ, Busch DH. *Inorg Chim Acta.* 2003; 346:76–86.
4. Hubin TJ. *Coord Chem Rev.* 2003; 241:27–46.
5. Yin G, Buchalova M, Danby AM, Perkins CM, Kitko D, Carter JD, Scheper WM, Busch DH. *J Am Chem Soc.* 2005; 127:17170–17171. [PubMed: 16332049]
6. Yin G, Danby AM, Kitko D, Carter JD, Scheper WM, Busch DH. *Inorg Chem.* 2007; 46:2173–2180. [PubMed: 17295471]
7. Yin G, Danby AM, Kitko D, Carter JD, Scheper WM, Busch DH. *J Am Chem Soc.* 2008; 130:16245–16253. [PubMed: 18998682]
8. Chattopadhyay S, Geiger RA, Yin G, Busch DH, Jackson TA. *Inorg Chem.* 2010; 49:7530–7535. [PubMed: 20690762]

9. Shi S, Wang Y, Xu A, Wang H, Zhu D, Roy SB, Jackson TA, Busch DH, Yin G. *Angew Chem Int Ed.* 2011; 50:7321–7324.
10. Wang Y, Shi S, Wang H, Zhu D, Yin G. *Chem Commun.* 2012; 48:7832–7834.
11. Wang Y, Sheng J, Shi S, Zhu D, Yin G. *J Phys Chem C.* 2012; 116:13231–13239.
12. Wang Y, Shi S, Zhu D, Yin G. *Dalton Trans.* 2012; 41:2612–2619. [PubMed: 22223076]
13. Dong L, Wang Y, Lu Y, Chen Z, Mei F, Xiong H, Yin G. *Inorg Chem.* 2013; 52:5418–5427. [PubMed: 23600453]
14. Yin G. *Acc Chem Res.* 2013; 46:483–492. [PubMed: 23194251]
15. Weisman GR, Rogers ME, Wong EH, Jasinski JP, Paight ES. *J Am Chem Soc.* 1990; 112:8604–8605.
16. Feng Y, England J, Que LJ. *ACS Catal.* 2011; 1:1035–1042.
17. Wainwright KP. *Inorg Chem.* 1980; 19:1396–1398.
18. Helps IM, Parker D, Murphy JR, Chapman J. *Tetrahedron.* 1989; 45:219–226.
19. Kolinski RA. *Polish J Chem.* 1995; 69:1039–1045.
20. Kowallick R, Neuburger M, Zehnder M, Kaden TA. *Helv Chem Acta.* 1997; 80:948–959.
21. Boiocchi M, Bonizzoni M, Fabbrizzi L, Foti F, Licchelli M, Poggi A, Taglietti A, Zema M. *Chem Eur J.* 2004; 10:3209–3216. [PubMed: 15224329]
22. Khan A, Silversides JD, Madden L, Greenman J, Archibald SJ. *Chem Commun.* 2007:416–418.
23. McRobbie G, Valks GC, Empson CJ, Khan A, Silversides JD, Pannecouque C, De Clercq E, Fiddy SG, Bridgeman AJ, Young NA, Archibald SJ. *Dalton Trans.* 2007:5008–5018. [PubMed: 17992286]
24. Silversides JD, Allan CC, Archibald SJ. *Dalton Trans.* 2007; 9:971–978. [PubMed: 17308678]
25. Plutnar J, Havlickova J, Kotek J, Hermann P, Lukes I. *New J Chem.* 2008; 32:496–504.
26. Boswell CA, Regino CAS, Baidoo KE, Wong KJ, Milenic DE, Kelley JA, Lai CC, Brechbiel MW. *Bioorg & Medicinal Chem.* 2009; 17:548–552.
27. Thibon A, England J, Martinho M, Young VGJ, Frisch JR, Guillot R, Girerd JJ, Munck E, Que LJ, Banse F. *Angew Chem Int Ed.* 2008; 47:7064–7067.
28. Alcock, NW.; Balakrishnan, KP.; Moore, P. *J Chem Soc. Dalton Trans;* 1986. p. 1743-1745.
29. Asato, E.; Hashimoto, S.; Matsumoto, N.; Kida, S. *J Chem Soc. Dalton Trans;* 1990. p. 1741-1746.
30. Vuckovic G, Asato E, Matsumoto N, Kida S. *Inorg Chim Acta.* 1990; 171:45–52.
31. Royal G, Dahaoui-Gindrey V, Dahaoui S, Tabard A, Guillard R, Pullumbi P, Lecomte C. *Eur J Org Chem.* 1998:1971–1975.
32. Bucher C, Royal G, Barbe JM, Guillard R. *Tetrahedron Lett.* 1999; 40:2315–2318.
33. Goeta, AE.; Howard, JAK.; Maffeo, D.; Puschmann, H.; Williams, JAG.; Yufit, DS. *J Chem Soc. Dalton Trans;* 2000. p. 1873-1880.
34. Batsanov AS, Goeta AE, Howard JAK, Maffeo D, Puschmann H, Williams JAG. *Polyhedron.* 2001; 20:981–986.
35. El Ghachtouli S, Cadiou C, Dechamps-Olivier I, Chuburu F, Aplincourt M, Roisnel T. *Eur J Inorg Chem.* 2006:3472–3481.
36. El Ghachtouli S, Cadiou C, Dechamps-Olivier I, Chuburu F, Aplincourt M, Patinec V, Le Baccon M, Handel H, Roisnel T. *New J Chem.* 2006; 30:392–398.
37. Narayanan J, Solano-Peralta A, Ugalde-Salvidar VM, Escudero R, Hopfl H, Sosa-Torres ME. *Inorg Chim Acta.* 2008; 361:2747–2758.
38. Morfin JF, Tripier R, Le Baccon M, Handel H. *Polyhedron.* 2009; 28:3691–3698.
39. Jones DG, Wilson KR, Cannon-Smith DJ, Shircliff AD, Zhan Z, Chen Z, Prior TJ, Yin G, Hubin TJ. *Inorg Chem.* 2015; 54:2221–2234. [PubMed: 25671291]
40. Almassio MF, Sarimbalis MN, Garay RO. *Designed Monomers and Polymers.* 2005; 8:287–296.
41. **Synthetic Details:** *3a*-(pyridin-2-ylmethyl)-decahydro-5*a,8a,10a*-triaza-3*a*-azoniapyrenium iodide (**5**). 13.28 g (0.08096 mol, 2 eq.) of picolyl chloride hydrochloride and 13.60 g (0.1619 mol, 4 eq.) of anhydrous NaHCO₃ were stirred in 700 ml chloroform for 1 h. Solids were removed by filtration and the filtrate was added to 9.00 g (0.04048 mol, 1 eq.) of (**4**) [52] and 13.44 g (0.08096 mol, 2 eq.) of KI. The reaction was stirred and heated to reflux for 6 d under nitrogen, during

which it became an orange color. After cooling, minimal solids were removed by filtration and discarded. The filtrate was evaporated to 100 ml volume and excess diethyl ether was added to precipitate the yellow solid product, which was filtered on a glass frit, washed with diethyl ether, and dried under vacuum. Yield = 11.841 g (66%). Electrospray mass spectrometry gave a single peak at $m/z = 314$ corresponding to $(M-I)^+$. Anal. Calc. for $C_{18}H_{28}N_5I \cdot H_2O$: C 47.06, H 6.58, N 15.25; found: C 46.87, H 6.54, N 14.88. 1H NMR (300 MHz, $CDCl_3$) δ 1.36 (d, 1H), 1.84 (d, 1H), 2.25 (m, 2H), 2.41 (d, 1H), 2.56 (d, 1H), 2.66 (m, 2H), 3.03 (m, 6H), 3.23 (t, 1H), 3.65 (m, 2H), 3.89 (d, 1H), 4.21 (m, 2H), 4.40 (td, 1H), 4.58 (s, 1H), 5.45 (m, 2H), 7.41 (m, 1H), 7.84 (m, 1H), 8.31 (d, 1H), 8.66 (d, 1H). $^{13}C\{^1H\}$ NMR (75.6 MHz, D_2O) δ 18.0, 18.4, 41.9, 46.6, 49.4, 51.3, 51.9, 53.2, 54.0, 60.5, 62.9, 69.5, 82.2, 125.8, 129.0, 138.6, 146.6, 150.3. *5-(pyridin-2-ylmethyl)-1,5,8,12-tetraazabicyclo[10.2.2]hexadecane (3)*. 14.138 g (0.0320 mol, 1 eq.) of **5** was stirred in 1 L of 95% EtOH in a 2 L roundbottom flask. 6.059 g (0.160 mol, 5 eq.) of $NaBH_4$ was added and the reaction was stirred at reflux for 1.5 h under N_2 . Upon cooling, 12 M HCl was added to a pH of 2. Solvent was removed under vacuum and the residue was dissolved in 100 ml of water to which 200 ml of 30% KOH was added. The cloudy white suspension was extracted into benzene, dried over Na_2SO_4 , and evaporated to a tan oil. Yield = 7.947 g (78%). Electrospray mass spectrometry gave a single peak at $m/z = 318$ corresponding to $(MH)^+$. Anal. Calc. for $C_{18}H_{31}N_5 \cdot 1.3H_2O \cdot 0.1C_6H_6$: C 64.07, H 9.89, N 20.08; found: C 63.80, H 10.00, N 19.87. 1H NMR (300 MHz, $CDCl_3$) δ 1.65 (m, 4H), 2.16 (m, 2H), 2.45-2.65 (m, 11H), 2.86 (m, 4H), 3.14 (m, 2H), 3.73 (s, 2H), 3.82 (m, 2H), 7.09 (m, 1H), 7.30 (t, 1H), 7.56 (t, 1H), 8.45 (d, 1H). $^{13}C\{^1H\}$ NMR (75.6 MHz, D_2O) δ 23.5, 26.1, 48.0, 48.1, 50.4, 51.0, 55.0, 55.1, 55.7, 56.9, 58.9, 121.8, 123.6, 135.9, 148.9, 159.1. X-ray quality crystals of the diprotonated salt $H_2\mathbf{3}^{2+}$ were grown from evaporation of the acetonitrile solvent from a complexation reaction of **3** with $FeCl_2$ which yielded, in addition to the complex product, a small amount of colorless crystals of $H_2\mathbf{3}Cl_2 \cdot 2 H_2O$. $[Fe(\mathbf{3})]Cl_2$: 0.317 g (0.001 mol) of (**3**) and 0.127 g anhydrous $FeCl_2$ were added to 10 ml of anhydrous acetonitrile in an inert atmosphere glovebox. The reaction was stirred at room temperature for 1 day during which the brown $FeCl_2$ beads dissolved and formed a yellow precipitate. This product was filtered on a glass frit, washed with ether, and allowed to dry open to the atmosphere of the glovebox. A second crop was obtained from partial evaporation of the filtrate followed by filtration of the additional yellow powder that precipitated. Combined Yield = 0.275 g (62%). Electrospray mass spectrometry (in MeOH/ H_2O) gave a peak at $m/z = 421$ corresponding to $(Fe(\mathbf{3})(OH)(OCH_3))^{2+}$. Anal. Calc. for $[Fe(C_{18}H_{31}N_5)]Cl_2 \cdot 0.5 H_2O$: C 47.70, H 7.12, N 15.45; found C 47.58, H 7.46, N 15.31. $[Mn(\mathbf{3})Cl]PF_6$ and $[Cu(\mathbf{3})][PF_6]_2$: The general procedure for $[Fe(\mathbf{3})]Cl_2$ above was followed, however, these reactions gave little or no precipitation. The solutions were filtered to remove trace solids, which were discarded. The filtrates were then evaporated under vacuum to give crude $[M(\mathbf{3})]$ chloride salts that was dissolved in a minimum MeOH in the glovebox. To these solutions were added 0.815 g (0.005 mol, 5 eq.) of NH_4PF_6 likewise dissolved in a minimum of MeOH. Precipitation of the PF_6 salt products was immediate, but the suspensions were allowed to stir approximately 1 h to complete precipitation. The solid products were filtered off, washed with diethyl ether, and allowed to dry overnight open to the glovebox atmosphere. $[Mn(\mathbf{3})Cl]PF_6$: Yield = 0.393 g (71%) of white powder. Electrospray mass spectrometry gave peaks at $m/z = 393$ corresponding to $Mn(\mathbf{3})(H_2O)^+$ and $m/z = 421$ corresponding to $(Mn(\mathbf{3})(CH_3OH)(H_2O))^+$. Anal. Calc. for $[Mn(C_{18}H_{31}N_5)Cl]PF_6 \cdot 3 H_2O$: C 35.62, H 6.15, N 11.54; found C 35.62, H 6.10, N 11.67. $[Cu(\mathbf{3})][PF_6]_2$ Yield = 0.457 g (68%) of blue powder. Electrospray mass spectrometry gave peaks at $m/z = 379$ corresponding to $(Cu(\mathbf{3}))^+$ and $m/z = 190$ corresponding to $(Cu(\mathbf{3}))^{2+}$. Anal. Calc. for $[Cu(C_{18}H_{31}N_5)][PF_6]_2 \cdot 0.2 H_2O$: C 32.05, H 4.69, N 10.38; found C 31.69, H 4.66, N 10.32. X-ray quality crystals were obtained from the diffusion of ether into an acetone solution.

42. Le Baccon M, Chuburu F, Toupet L, Handel H, Soibinet M, Deschamps-Olivier I, Barbier JP, Aplincourt M. *New J Chem.* 2001; 25:1168–1174.
43. **X-ray Crystallographic Details:** Single crystal X-ray diffraction data were collected in series of ω -scans using a Stoe IPSD2 image plate diffractometer utilising monochromated Mo radiation ($\lambda = 0.71073 \text{ \AA}$). Standard procedures were employed for the integration and processing of the data using X-RED. [53] Samples were coated in a thin film of perfluoropolyether oil and mounted at the tip of a glass fibre located on a goniometer. Data were collected from crystals held at 150 K in an Oxford Instruments nitrogen gas cryostream. Crystal structures were solved using routine automatic direct methods implemented within SHELXS-97. [54] Completion of structures was

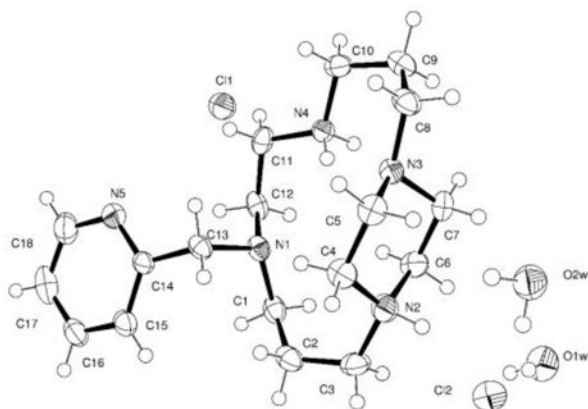
achieved by performing least squares refinement against all unique F² values using SHELXL-97. [54] All non-H atoms were refined with anisotropic displacement parameters. Hydrogen atoms were placed using a riding model. Where the location of hydrogen atoms was obvious from difference Fourier maps, C-H bond lengths were refined subject to chemically sensible restraints. Crystal Data for H₂3Cl₂ • 2 H₂O: C₁₈H₃₇N₅Cl₂O₂, *M_r* = 426.42, *Z* = 4, *T* = 150(2) K, Monoclinic, *P* 2₁/c, *a* = 17.1551(16) Å, *b* = 10.2884(11) Å, *c* = 13.0825(11) Å, α = 90°, β = 100.328(7)°, γ = 90°, *V* = 2271.6(4) Å³, *F*(000) = 920, GOF = 0.822. A total of 12083 reflections were collected, of which 4630 were unique (*R*(int)) = 0.0828). *R*₁ (*I* > 2σ(*I*)) = 0.0421, *wR*₂ = 0.1297. Crystal Data for [Cu(3)][PF₆]₂ • C₃H₆O: Cu₂C₃₉H₆₈N₁₀OP₄F₂₄, *M_r* = 1399.99, *Z* = 4, *T* = 150(2) K, Orthorhombic, *P* c a 21, *a* = 17.6639(8) Å, *b* = 9.8148(5) Å, *c* = 31.3088(18) Å, α = 90°, β = 90°, γ = 90°, *V* = 5427.6(4) Å³, *F*(000) = 2856, GOF = 0.798. A total of 33224 reflections were collected, of which 9229 were unique (*R*(int)) = 0.0554). *R*₁ (*I* > 2σ(*I*)) = 0.0318, *wR*₂ = 0.0569.

44. X-Area v 1.64. Darmstadt: STOE & Cie GmbH; 2012.
45. Sheldrick G. *Acta Crystallogr Sect A: Found Crystallogr.* 2008; 64:112–122.
46. Burger, K. *Coordination Chemistry: Experimental Methods.* London: Butterworth; 1973.
47. Barefield KE, Busch DH, Nelson SM. *Quart Rev Chem Soc.* 1968; 22:457–498.
48. Collinson SR, Alcock NW, Hubin TJ, Busch DH. *Journal of Coordination Chemistry.* 2001:317–331.
49. El Hajj F, Sebki G, Patinec V, Marchivie M, Triki S, Handel H, Yefsah S, Tripier R, Gomez-Garcia C, Coronado E. *Inorg Chem.* 2009; 48:10416–10423. [PubMed: 19780566]
50. Di Vaira M, Midollini S, Sacconi L. *Inorg Chem.* 1977; 1518–1524:16.
51. Sacconi L, Di Vaira M. *Inorg Chem.* 1978; 17:810–815.
52. Bianchini C, Laschi F, Masi D, Ottavianci FM, Pastor A, Peruzzini M, Zanello M, Zanello P, Zanobini F. *J Am Chem Soc.* 1993; 115:2723–2730.
53. Divaira M, Stoppioni PMJA. *Gazzetta Chimica Italiana.* 1995; 125:277–281.
54. Hubin TJ, Alcock NW, Morton MD, Busch DH. *Inorg Chim Acta.* 2003; 348:33–40.
55. Goldsmith CR, Stack TDP. *Inorg Chem.* 2006; 45:6048–6055. [PubMed: 16842013]
56. McGinley CM, van der Donk WA. *Chem Commun.* 2003:2843–2846.

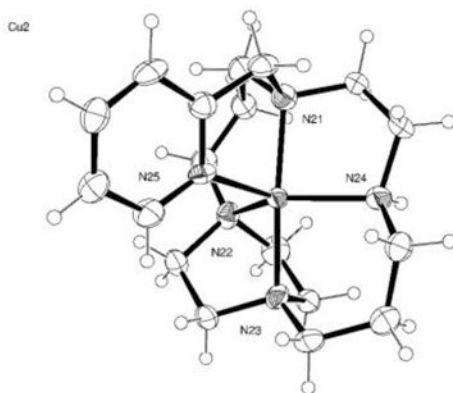
Research Highlights

- The first 2-pyridylmethyl side-bridge cyclam ligand and its X-ray crystal structure
- The first transition metal complex of a 2-pyridylmethyl side-bridge cyclam ligand and its X-ray crystal structure
- Cyclic voltammetry and oxidation screening of Mn^{2+} , Fe^{2+} , and Cu^{2+} complexes of this new ligand showing promising hydrogen atom abstraction for the Fe^{2+} complex

(a)



(b)



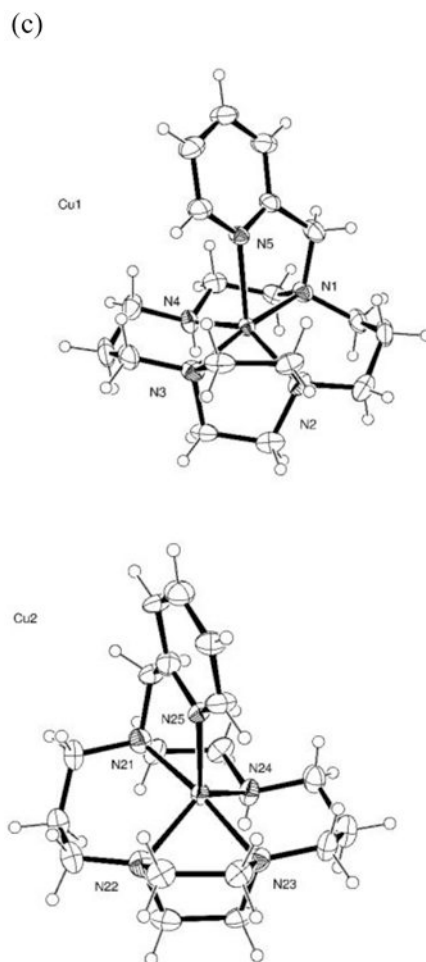


Figure 1. (a) Structure of $\text{H}_2\text{3Cl}_2 \cdot 2 \text{H}_2\text{O}$ (b) Structure of $\text{Cu}(\mathbf{3})^{2+}$ depicted as an approximate trigonal bipyramidal geometry (c) Structure of $\text{Cu}(\mathbf{3})^{2+}$ depicted as an approximate square-based pyramidal geometry and showing that the two slightly different ligand orientations are approximately enantiomers.

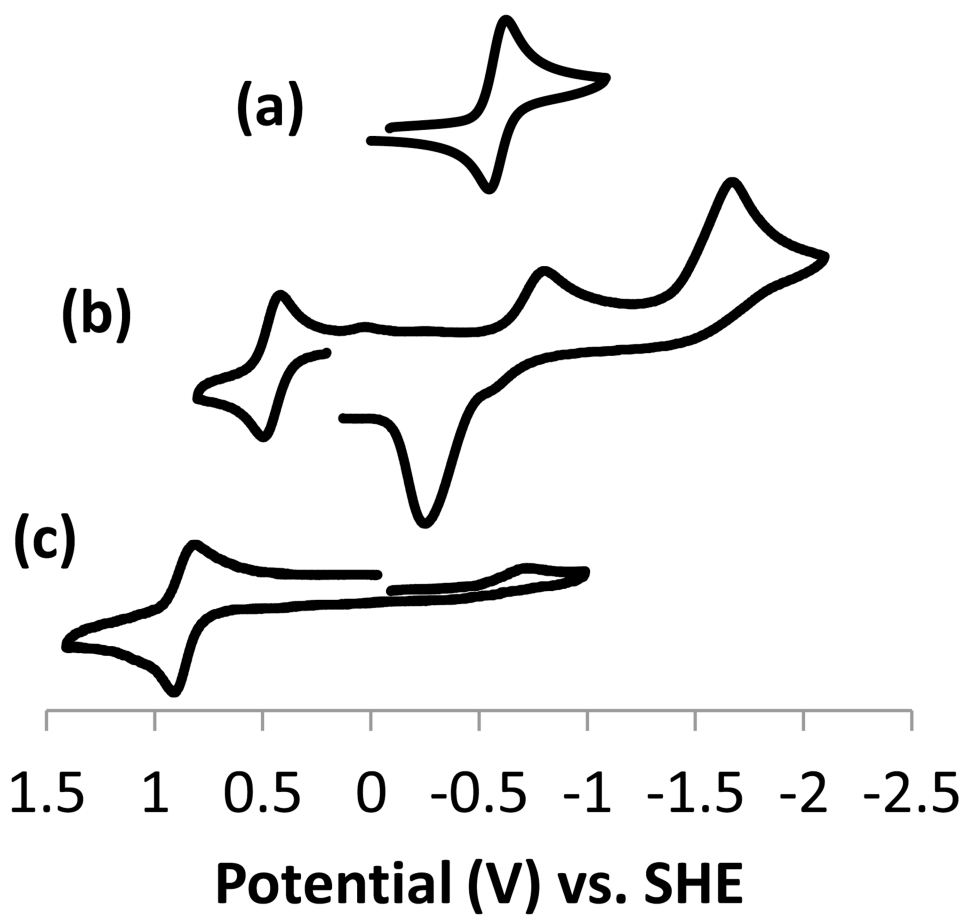
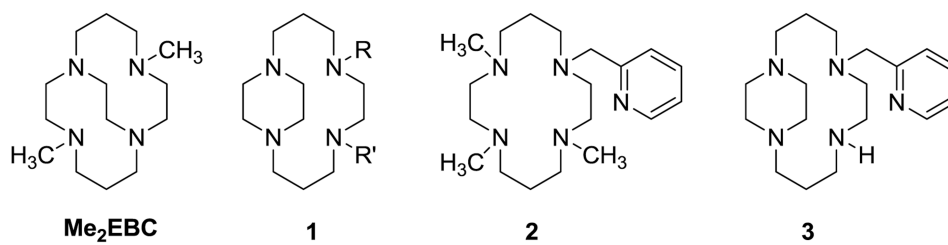
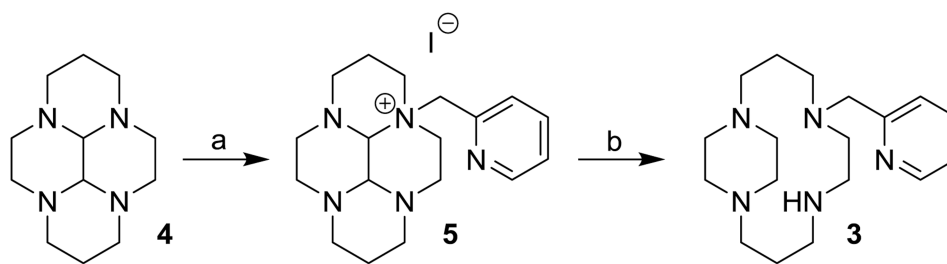


Figure 2. Cyclic voltammograms in acetonitrile vs. SHE for (a) Cu(III)^{2+} , (b) Fe(III)^{2+} , and (c) Mn(III)Cl^+ .



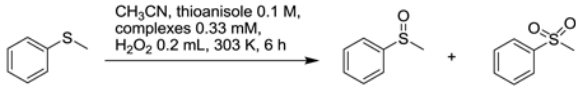
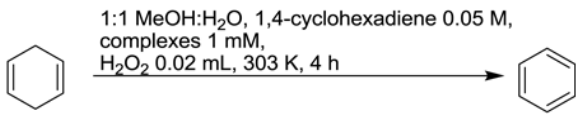
Scheme 1.
Ligands discussed in this paper.

**Scheme 2.**

Synthesis of **3**. a) i. CHCl_3 , 2 eq. picolyl chloride hydrochloride, 4 eq. NaHCO_3 , 1 h, filter to remove solids; ii. 1 eq. of (**1**), 2 eq. KI, reflux 6 d; b) i. 95% EtOH, 5 eq. NaBH_4 , N_2 , reflux, 1.5 h; ii. 12 M $\text{HCl}(\text{aq})$, 30% $\text{KOH}(\text{aq})$, benzene extraction.

Table 1

Oxidation catalysis screening results for manganese(II), iron(II), and copper(II) complexes of **3**, in comparison to $\text{Mn}(\text{Me}_2\text{EBC})\text{Cl}_2$.

			
Complex	Conversion %	Yield % Sulfoxide	Yield % Sulfone
$\text{Mn}(\text{Me}_2\text{EBC})\text{Cl}_2$	99.8	44.3	46.5
$[\text{Mn}(\mathbf{3})\text{Cl}]^+$	8.3	0.2	0.02
$[\text{Fe}(\mathbf{3})]^{2+}$	15.6	9.7	2.9
$[\text{Cu}(\mathbf{3})]^{2+}$	6.1	3.4	1.9
			
Complex	Conversion %	Yield % Benzene	
$\text{Mn}(\text{Me}_2\text{EBC})\text{Cl}_2$	86.2	71.4	
$[\text{Mn}(\mathbf{3})\text{Cl}]^+$	23.1	3.5	
$[\text{Fe}(\mathbf{3})]^{2+}$	44.5	23.6	
$[\text{Cu}(\mathbf{3})]^{2+}$	29.6	4	